Vacuum polarization in the spacetime of charged nonlinear black hole

Waldemar Berej* and Jerzy Matyjasek†

Institute of Physics, Maria Curie-Skłodowska University,

pl. Marii Curie-Skłodowskiej 1,

20-031 Lublin, Poland

Abstract

Building on general formulas obtained from the approximate renormalized effective action, the approximate stress-energy tensor of the quantized massive scalar field with arbitrary curvature coupling in the spacetime of charged black hole being a solution of coupled equations of nonlinear electrodynamics and general relativity is constructed and analysed. It is shown that in a few limiting cases, the analytical expressions relating obtained tensor to the general renormalized stress-energy tensor evaluated in the geometry of the Reissner-Nordström black hole could be derived. A detailed numerical analysis with special emphasis put on the minimal coupling is presented and the results are compared with those obtained earlier for the conformally coupled field. Some novel features of the renormalized stress-energy tensor are discussed.

PACS numbers: 04.70.Dy, 04.62+v

I. INTRODUCTION

One of the most intriguing open questions in modern theoretical physics is the issue of a final stage of the black hole evaporation. Although a definite answer would be possible only with the full machinery of quantum theory of gravity, some important preliminary results may be, in principle, obtained within the framework of semiclassical theory. However, as the semiclassical approach could not be used to describe the evolution of the system in the Planck regime, it can, at best, tell us about a tendency rather than the limit itself. Unfortunately,

*Electronic Address: berej@tytan.umcs.lublin.pl

†Electronic Address: matyjase@tytan.umcs.lublin.pl, jurek@kft.umcs.lublin.pl

even this simplified programme is hard to execute as the semiclassical Einstein field equations comprise a rather complicated set of nonlinear partial differential equations, and, moreover, the source term — the renormalized stress-energy tensor — should be known for a wide class of nonstatic metrics. It is natural, therefore, that in order to make the back reaction problem tractable, one should refer to some approximations.

It seems that the most promising approach consists in constructing the approximate stress-energy tensor in the geometry of a static black hole and subsequent computation of the semiclassical corrections to the classical metric. Although evaluated in the static background, such corrections, as has been pointed out in Ref. [1], are relevant because they give direct information about the influence of the quantum effects on the temperature of a black hole. Thus far this programme, initiated in Ref. [2], has been carried out for massless fields in Schwarzschild spacetime [3–8] and for massive scalar fields with arbitrary curvature coupling in Reissner-Nordström (RN) geometry [1], where, among other things, quantum corrections to the geometry, entropy, and trace anomaly were computed. The most important ingredient of the approach is therefore the renormalized stress-energy tensor of the quantized field propagating in a spacetime of the static black hole constructed in a physically interesting state. However, direct evaluation of this object is rather complicated.

It is believed that the physical content of the theory of quantum fields in curved spacetime is contained in the (renormalized) effective action, W_R, a useful quantity allowing evaluation of the stress-energy tensor by means of the standard formula

$$\frac{2}{g^{1/2}}\frac{\delta}{\delta g_{ab}}W_{ren} \,=\, \langle T^{ab}\rangle_{ren}. \tag{1}$$

Unfortunately, the effective action is a nonlocal functional of the metric and its exact form is unknown. In the attempts to construct the renormalized stress-energy tensor one is forced, therefore, to employ numerical methods or to accept some approximations.

For the quantized massive fields in the large mass limit, i.e. when the Compton length is much smaller than the characteristic radius of a curvature, the nonlocal contribution to the effective action can be neglected, and the series expansion in m^{-2} of the renormalized effective action, W_R, may be constructed with the aid of the DeWitt-Schwinger method [9–11]. Thus constructed renormalized effective action has the form

$$W_{ren} \,=\, \frac{1}{32\pi^2 m^2}\int d^4x\, g^{1/2}\sum_{n=3}^{\infty}\frac{(n-3)!}{(m^2)^{n-2}}[a_n(x,x')], \tag{2}$$

where $[a_n(x,x')]$ is a coincidence limit of the n-th Hadamard-Minakshisundaram-DeWitt-Seely (HMDS) coefficient. The coefficients are local, geometrical objects constructed from curvature tensor and its covariant derivatives of rapidly growing complexity. So far, only coefficients for $n \leq 4$ are known, but it seems the effective action constructed from higher order terms would be practically intractable, especially in the attempts to calculate the stress-energy tensor.

The first nonvanishing term of the effective action constructed for the massive scalar field with arbitrary curvature coupling satisfying

$$\left(-\Box \,+\, \xi R \,+\, m^2\right)\phi \,=\, 0, \tag{3}$$

where ξ is the coupling constant and m is the mass of the field, form the coincidence limit of the HMDS coefficient $[a_3]$, is given by [12–14]:

$$
\begin{aligned}
W^{(1)}_{ren} \;=\; & \frac{1}{192\pi^2 m^2}\int d^4x g^{1/2}\left[\frac{1}{2}\left(\eta^2-\frac{\eta}{15}-\frac{1}{315}\right)R\Box R \;+\; \frac{1}{140}R_{pq}\Box R^{pq}\right.\\
& -\eta^3 R^3 \;+\; \frac{1}{30}\eta R R_{pq}R^{pq} \;-\; \frac{1}{30}\eta R R_{pqab}R^{pqab}\\
& -\frac{8}{945}R^p_q R^q_a R^a_p \;+\; \frac{2}{315}R^{pq}R_{ab}R^{a\ b}_{p\ q} \;+\; \frac{1}{1260}R_{pq}R^p_{\ cab}R^{qcab}\\
& \left.+\;\frac{17}{7560}R_{ab}^{\ \ pq}R_{pq}^{\ \ cd}R_{cd}^{\ \ ab} \;-\; \frac{1}{270}R^{a\ b}_{p\ q}R^{p\ q}_{c\ d}R^{c\ d}_{a\ b}\right]\\
= & \frac{1}{192\pi^2 m^2}\sum_{i=1}^{10}\alpha_i W_{(i)},
\end{aligned}
\tag{4}
$$

where $\eta=\xi-1/6$ and α_i are numerical coefficients that stand in front of geometric terms in $W^{(1)}_{ren}$. Differentiating functionally $W^{(1)}_{ren}$ with respect to a metric tensor one obtains

$$
\begin{aligned}
\langle T^{ab}\rangle &= \sum_{i=1}^{10}\alpha_i\tilde{T}^{(i)ab} = \frac{1}{96\pi^2 m^2 g^{1/2}}\sum_{i=1}^{10}\alpha_i\frac{\delta W_{(i)}}{\delta g_{ab}}\\
&= T^{(0)ab}+\eta T^{(1)ab}+\eta^2 T^{(2)ab}+\eta^3 T^{(3)ab},
\end{aligned}
\tag{5}
$$

where each $\tilde{T}^{(i)ab}$ is rather complicated expression constructed from the curvature tensor, its covariant derivatives, and contractions. Such calculations have been undertaken in Refs. [15,16], where generic expressions for the first nonvanishing order of the renormalized stress-energy tensor were obtained. They generalize earlier results of Frolov and Zel'nikov for vacuum type-D geometries [11]. One can easily extend this result to the case of spinor and vector field as the analogous expressions differ only by numerical coefficients α_i.

It should be emphasised, however, that the above assumptions place severe limitations on the domain of validity of the obtained approximation. Especially, it would be meaningless, at least in this formulation, to consider the massless limit of the approach. Therefore, the result, which consists of approximately one hundred local geometrical terms, may be used in any spacetime provided the temporal changes of the background geometry are slow and the mass of the field is sufficiently large. Because of the complexity of the thus obtained tensor it will be not presented here, and for its full form and technical details the reader is referred to [16].

For quantized massive scalar fields with arbitrary curvature coupling in static and spherically-symmetric geometries there exists a different method invented by Anderson, Hiscock, and Samuel [17]. Their calculations were based on the WKB approximation of the solutions of the radial equation and summation of thus obtained mode functions. Both methods are equivalent: to obtain the term proportional to m^{-2} one has to use 6-th order WKB, and explicit calculations carried out for the Reissner-Nordström spacetime as well as in wormhole geometries considered in Ref. [18] yielded identical results. Moreover, detailed numerical analyses carried out in Ref. [17] and briefly reported in [1] show that for $mM \gtrsim 2$ (M being the black hole mass), the accuracy of the Schwinger-DeWitt approximation in the Reissner-Nordström geometry is quite good (1% or better).

Geometry of the Reissner-Nordström black hole is singular as $r \to 0$ and there is a natural desire to construct its regular generalizations. It is expected that a good candidate for the source term of the Einstein equations is the (classical) stress-energy tensor of nonlinear electrodynamics. Moreover, renewal of interests in nonlinear electrodynamics that is seen recently is motivated by the observation that such theories arose as limiting cases of certain formulations of string theory. Unfortunately, the no go theorem proved in Ref. [19] clearly shows that for Lagrangians $\mathcal{L}(F)$, $(F = F_{ab}F^{ab})$, with the Maxwell weak-field limit there are no spherically-symmetric static black hole solutions with a regular center.

Recently, employing the Schwinger-DeWitt approximation we have constructed the renormalized stress-energy tensor of the quantized conformally coupled massive scalar field in the spacetime of the electrically charged regular black hole being an exact solution of the equations of the nonlinear electrodynamics and the Einstein field equations. Such a solution has been proposed by Ayón-Beato and García (ABG) in Ref. [20]. It should be noted, however, the ABG line element is not a solution of the standard nonlinear electrodynamics and the effective geometry (i.e. the geometry seen by photons of the nonlinear theory) is singular. Fortunately, the ABG solution may be reinterpreted as describing a magnetically charged regular solution of the coupled equations of standard nonlinear electrodynamics and gravitation with much more regular behaviour of the effective geometry [21]. Moreover, it has been shown recently that it is possible to combine electric and magnetic line elements to obtain a regular electric solution with a magnetic core [22].

For small and intermediate charges as well as at large distances, the geometry of the ABG black hole resembles that of RN; noticeable differences appear near the extremality limits. It is interesting therefore to analyse how the similarities in the metric structure of the ABG and RN black holes are reflected in the structure of the stress-energy tensors. As for the conformally coupled massive scalar field the linear, quadratic, and cubic terms in η in the stress-energy tensor (5) are absent, it is anticipated that such similarities do occur. Explicit calculations carried out in [16] confirmed this hypothesis and showed that for small values of q the appropriate tensors are practically indistinguishable, and, as expected, important differences appear near and at the extremality limit.

In this paper we shall extend the results of Ref. [16] and investigate a much more complicated case of arbitrary η with special emphasis put on the minimal coupling. Although complexity of the approximate stress-energy tensor constructed for the ABG line element practically prevents its direct examination, it is possible to extract interesting information expanding $\langle T_a^b \rangle$ into a power series and retaining a few leading terms. We shall show that such analyses could be carried out for small charges, large distances, and in the vicinity of the event horizon of the extremal ABG black hole. Moreover, on general grounds one may easily estimate the role played by $\tilde{T}^{(1)ab}$ and $\tilde{T}^{(3)ab}$. To gain a deeper understanding of the problem, however, we employ numerical calculations.

The paper is organized as follows. In Sec. II the essentials of the ABG black hole geometry that are neccessary in further development are briefly described. In Sec. III certain features of the approximate stress-energy tensor of the massive scalar field in the ABG geometry are discussed and compared with the appropriate tensors constructed in the RN geometry. The results of our numerical analyses are presented in Sec. IV in which we discuss behaviour of the components of $\langle T_a^b \rangle$ in some detail and present it graphically.

II. GEOMETRY

The general Reissner-Nordström solution of the Einstein-Maxwell equations describing a static and spherically symmetric black hole of mass M, electric charge e, and magnetic monopole charge e_m has a remarkably simple form

$$ds^2 = -A(r)\,dt^2 + A^{-1}(r)\,dr^2 + r^2\left(d\theta^2 + \sin^2\theta d\phi^2\right), \tag{6}$$

with

$$A(r) = 1 - \frac{2M}{r} + \frac{e^2 + e_m^2}{r^2}. \tag{7}$$

Since the charges enter (7) as a sum of squares the metric structure remains unchanged under the changes of charges leaving $Q^2 = e^2 + e_m^2$ constant. For $Q^2/M^2 < 1$, the equation $A(r) = 0$ has two positive roots

$$r_\pm = M \pm \sqrt{M^2 - Q^2}, \tag{8}$$

and the larger one, r_+, determines the location of the event horizon, whereas the smaller, r_-, gives the position of the inner horizon. In the limit $Q^2 = M^2$ horizons merge at $r = M$ and the black hole degenerates to the extremal one. At $r = 0$ the Reissner-Nordström solution has an irremovable curvature singularity, which, although hidden to an external observer for $Q^2/M^2 \leq 1$, remains a somewhat unwanted feature of the solution. The solution for $Q^2 > M^2$ is clearly unphysical.

At least for purely electrical solutions the nonlinear electrodynamics does not remedy the situation. Indeed, consider ralization of the nonlinear electrodynamics with the action functional of the form

$$S = \frac{1}{16\pi}\int d^4x\sqrt{-g}\left[R - \mathcal{L}(F)\right], \tag{9}$$

where R is a curvature scalar, $F = F_{ab}F^{ab}$, and $\mathcal{L}(F)$ is an arbitrary function with Maxwell asymptotic in a weak field limit, i. e. $\mathcal{L}(F) \to F$ and $\frac{d}{dF}\mathcal{L}(F) \to 1$ as $F \to 0$. According to a well known theorem [19,21], there are no regular, static, and spherically symmetric solutions of general relativity coupled to nonlinear electrodynamics describing a black hole with nonzero electric charge. However, as has been explicitly demonstrated recently by Bronnikov, adopted hypotheses leave room for appropriate regular solutions with a nonzero *magnetic* charge. In this regard it is interesting to note that within a different formulation of the nonlinear electrodynamics proposed in [23] (a $\mathcal{P}$ framework according to the nomenclature of Refs. [24,21]) obtained from the standard one (the $\mathcal{F}$ formulation) (9) by means of a Legendre transformation, Ayón-Beato and García constructed a regular black hole solution with a nonzero electric charge and mass [20]. Their solution has the simple form (6), where

$$A(r) = 1 - \frac{2M}{r}\left(1 - \tanh\frac{e^2}{2Mr}\right). \tag{10}$$

Bronnikov also demonstrated that any spherically symmetric solution constructed within the $\mathcal{F}$ framework has its counterpart with the same metric tensor constructed within the

$\mathcal{P}$ framework, and therefore the electric solution (6) has the magnetic companion with e replaced by the magnetic charge e_m. Moreover, Burinskii and Hildebrandt have proposed recently a regular hybrid model in which electrically and magnetically charged solutions were combined in such a way that the electric field does not extend to the center of the black hole [22].

Although the magnetic and electric ABG solutions are precisely of the type (6) with (10), the geometries seen by photons of the nonlinear theory are different. It is because photons of the nonlinear theory move along null geodesics of the effective metric, and the latter is singular for the electric solution [25–27]. It should be noted, however, that otherwise the physical geometry is regular and well behaving.

Since geometries outside the event horizon are described by the same line element and since we are going to consider neutral scalar field only, our results will hold for any particular realization of the ABG black hole as the only concern here is the metric structure of the spacetime. Therefore in what follows we denote both electric and magnetic charge by e.

Inspection of the metric potentials reveals interesting features of the ABG solution: its curvature invariants are finite as $r \to 0$ and at large r it approaches the Reissner-Nordström solution. Moreover, for small and intermediate values of the ratio e^2/M^2, the radial coordinate of the event horizon, r_+, is close to the event horizon of the RN black hole; significant differences occur near the extremality limit.

It has been shown in [16] that the location of the horizons of the ABG black hole may be expressed in terms of the Lambert function W [28]. Indeed, making use of the substitution $r = Mx$, $e^2 = q^2M^2$, it could be demonstrated that the location of the horizons is given by the real branches of the Lambert functions:

$$x_{\pm} = -\frac{4q^2}{4W(\varepsilon, -q^2/4\,\exp(q^2/4)) - q^2}, \tag{11}$$

where ε is 0 for the event horizon, x_+ , and -1 for the inner one, x_-. The functions $W(0, s)$ and $W(-1, s)$ are the only real branches of the Lambert function with the branch point at $s = -\mathrm{e}^{-1}$, where e is the base of natural logarithms and

$$W(0, -\mathrm{e}^{-1}) = W(-1, -\mathrm{e}^{-1}) = -1. \tag{12}$$

Consequently, for

$$q = 2\sqrt{w} \tag{13}$$

the horizons merge at

$$x_{extr} = \frac{4w}{1+w}, \tag{14}$$

where $w = W\left(0, \mathrm{e}^{-1}\right) = 0.2785$. Numerically, one has $x_{extr} = 0.871$ for $|e|/M = 1.055$.

For small values of q, the ABG line element resembles that of RN. Indeed, expanding the function $A(x)$ one has

$$A(x) = 1 - \frac{2}{x} + \frac{q^2}{x^2} + \mathcal{O}\left(q^4\right). \tag{15}$$

In spite of similarities between ABG and RN geometries for $q \ll 1$, there are substantial differences in the extremality limit: the extremal RN line element is described by (6) with

$$A(x) \,=\, \left(1-\frac{1}{x}\right)^2, \tag{16}$$

whereas near the event horizon of the extremal ABG black hole the function $A(x)$ has the following expansion

$$A(x) \,=\, (x-x_{extr})^4 \,+\, \frac{(1+w)^3}{32w^2}(x-x_{extr})^5 \,+\, O(x-x_{extr})^6. \tag{17}$$

The form of the above expansion indicates that the proper length between the event horizon and any point located at $r > r_{extr}$ is infinite.

III. THE RENORMALIZED STRESS-ENERGY TENSOR

Structure of terms in the effective potential (4) and in Eq. (5) indicates that for the conformally coupled massive scalar field, i.e. for $\eta = 0$, there are substantial simplifications of the renormalized stress-energy tensor as in this very case the third, fourth, and fifth term in (4) do not contribute to the final result. Moreover, from (4) it is evident that in $R = 0$ geometries and for arbitrary curvature coupling the functional derivative of the first and the third terms in (4) with respect to the metric tensor vanishes and, therefore, the approximate renormalized stress-energy tensor of the massive field in RN spacetime has a general form

$$T_a^b = C_a^b + \eta D_a^b. \tag{18}$$

On the other hand, however, for the ABG metric one has

$$R = \frac{q^4}{M^2x^5}\tanh\left(\frac{q^2}{2x}\right)\left[1-\tanh^2\left(\frac{q^2}{2x}\right)\right], \tag{19}$$

which for small q is $\mathcal{O}\left(q^6\right)$. Detailed calculations carried out for $q \ll 1$ show that for the ABG solution neither $\tilde{T}_a^{(1)b}$ nor $\tilde{T}_a^{(3)b}$ contribute importantly to the result.

Because of the similarities of the metric structure of the RN and ABG solutions, the overall behaviour of the renormalized stress-tensors for conformal coupling should be qualitatively similar and comparable in magnitude at least for small and intermediate values of q. However, the differences between the line element (16) and the expansion (17), give strong evidence for differences in the appropriate components of the approximate stress-energy tensors. For the conformally coupled massive scalar field this statement has been confirmed by extensive numerical calculations reported in Ref. [16]. Now we shall analyse the case of an arbitrary coupling with curvature. First, observe that contribution of $\eta^2\tilde{T}^{(1)ab}$ and $\eta^3\tilde{T}^{(3)ab}$ to the stress-energy tensor could be made arbitrarily great by a suitable choice of the conformal coupling. It should be noted, however, that such great values of η are clearly unphysical and should be rejected. Therefore, as the particular case of the conformal coupling has been considered earlier, here we shall confine ourselves mostly to the important and physically interesting case of minimal coupling $\eta = -1/6$.

In order to construct C_a^b and D_a^b one has to either calculate the curvature tensor and its covariant derivatives to required order for the line element (6) with (7) and employ the general formulas presented in [15] or to make use of the method proposed by Anderson, Hiscock and Samuel [17]. Both approaches yield the same result, which reads:

$$C_t^t = \frac{810\,x^4q^2 - 855\,x^4 - 202\,x^2q^4 + 1878\,x^3 - 1152\,x^3q^2 - 2307\,x^2q^2 + 3084\,xq^4 - 1248\,q^6}{30240M^6\pi^2m^2x^{12}}, \tag{20}$$

$$D_t^t = \frac{-1008\,x^3q^2 + 819\,q^6 + 2604\,x^2q^2 + 728\,x^2q^4 - 2712\,xq^4 + 360\,x^4 - 792\,x^3}{720M^6\pi^2m^2x^{12}}, \tag{21}$$

$$C_t^t = \frac{842\,x^2q^4 + 444\,q^6 + 162\,x^4q^2 - 462\,x^3 - 1488\,x^3q^2 - 1932\,xq^4 + 315\,x^4 + 2127\,x^2q^2}{30240M^6\pi^2m^2x^{12}}, \tag{22}$$

$$D_r^r = \frac{504\,xq^4 - 208\,x^2q^4 - 588\,x^2q^2 + 336\,x^3q^2 - 117\,q^6 + 216\,x^3 - 144\,x^4}{720M^6\pi^2m^2x^{12}}, \tag{23}$$

$$C_\theta^\theta = \frac{2202\,x^3 - 486\,x^4q^2 - 945\,x^4 - 3044\,x^2q^4 + 4884\,x^3q^2 - 9909\,x^2q^2 + 10356\,xq^4 - 3066\,q^6}{30240M^6\pi^2m^2x^{12}} \tag{24}$$

and

$$D_\theta^\theta = \frac{-1176\,x^3q^2 + 1053\,q^6 + 3276\,x^2q^2 + 832\,x^2q^4 - 3408\,xq^4 + 432\,x^4 - 1008\,x^3}{720M^6\pi^2m^2x^{12}}. \tag{25}$$

The analogous tensor in the ABG geometry is more complicated, and besides the linear terms it contains also terms which are quadratic and cubic in η. Each component of the stress-energy tensor consists of more than three hundred terms and has a general form

$$\frac{1}{96\pi^2m^2M^6}\left(1 - \tanh\frac{q^2}{2x}\right)\sum_{i,j,k}\alpha_{ijk}\frac{q^{2i}}{x^j}\tanh^k\frac{q^2}{2x}, \tag{26}$$

where α_{ijk} for a given η are numerical coefficients ($0 \leq i \leq 6$, $8 \leq j \leq 15$, $0 \leq k \leq 8$), and for obvious reasons will not be presented here.

Since the form of the Eq. (26) differs considerably from the stress-energy tensor given by (18) with (20–25), it could be expected that the runs of both tensors have nothing in common. On the other hand similarities in the metric structure of the RN and ABG black holes discussed earlier strongly suggest the opposite. Unfortunately, the complexity of the renormalized stress-energy tensor of the massive scalar field in the ABG geometry practically invalidates direct analytical treatment. One can, however, obtain interesting and important information analysing certain limiting cases. Indeed, expanding the stress-energy tensor for $q \ll 1$ one has

$$\langle T_a^b \rangle^{ABG} = T_a^b + \Delta_a^{(1)b} + \mathcal{O}\left(q^8\right), \tag{27}$$

where T_a^b is given by (18–25) and

$$96\pi^2 m^2 \Delta_t^{(1)t} = -\frac{q^6\ (12049 - 11416\,x + 2660\,x^2)}{420\,M^6\,x^{12}} + \frac{2\,q^6\ (617 - 596\,x + 140\,x^2)\ \eta}{5\,M^6\,x^{12}} - \frac{12\,q^6\ (459 - 366\,x + 70\,x^2)\ \eta^2}{M^6\,x^{12}}, \tag{28}$$

$$96\pi^2 m^2 \Delta_r^{(1)r} = -\frac{q^6\ (1555 - 1064\,x + 140\,x^2)}{420\,M^6\,x^{12}} - \frac{2\,q^6\ (121 - 140\,x + 40\,x^2)\ \eta}{5\,M^6\,x^{12}} + \frac{12\,q^6\ (81 - 84\,x + 20\,x^2)\ \eta^2}{M^6\,x^{12}}, \tag{29}$$

$$96\pi^2 m^2 \Delta_\theta^{(1)\theta} = \frac{q^6\ (5249 - 3528\,x + 560\,x^2)}{420\,M^6\,x^{12}} + \frac{2\,q^6\ (779 - 720\,x + 160\,x^2)\ \eta}{5\,M^6\,x^{12}} - \frac{12\,q^6\ (540 - 423\,x + 80\,x^2)\ \eta^2}{M^6\,x^{12}}. \tag{30}$$

Inspection of expansions (28–30), which are valid for any η and x, shows that in this order the term $\tilde{T}^{ab}_{(3)}$ is absent in the final result. It is because $\tilde{T}_a^{(3)b} \sim \mathcal{O}\left(q^{12}\right)$. The second term $\tilde{T}_a^{(1)b}$, which vanishes in the RN geometry is now $\mathcal{O}\left(q^6\right)$.

A similar expansion valid for large values of radial coordinate has the following form

$$\langle T_a^b \rangle^{ABG} = T_a^b + \Delta_a^{(1)b} + \Delta_a^{(2)b} + \mathcal{O}\left(x^{-13}\right), \tag{31}$$

where T_a^b is given by (18–25), $\Delta_a^{(1)b}$ by (28–30), and

$$96\pi^2 m^2 \Delta_t^{(2)t} = \frac{q^8\ (-2574 + 1015\,q^2)}{210\,M^6\,x^{12}} - \frac{14\,q^8\ (-39 + 20\,q^2)\ \eta}{5\,M^6\,x^{12}} + \frac{105\,q^8\ (-27 + 8\,q^2)\ \eta^2}{M^6\,x^{12}}, \tag{32}$$

$$96\pi^2 m^2 \Delta_r^{(2)r} = \frac{q^8\ (-738 + 35\,q^2)}{378\,M^6\,x^{12}} + \frac{4\,q^8\ (-51 + 28\,q^2)\ \eta}{9\,M^6\,x^{12}} - \frac{5\,q^8\ (-333 + 112\,q^2)\ \eta^2}{3\,M^6\,x^{12}}, \tag{33}$$

$$96\pi^2 m^2 \Delta_\theta^{(2)\theta} = \frac{q^8\ (12456 - 875\,q^2)}{1890\,M^6\,x^{12}} - \frac{112\,q^8\ (-12 + 5\,q^2)\ \eta}{9\,M^6\,x^{12}} + \frac{5\,q^8\ (-1989 + 560\,q^2)\ \eta^2}{3\,M^6\,x^{12}}. \tag{34}$$

Note that in Eqs. (32–34) there is no contribution from the term $\tilde{T}_a^{(3)b}$ and, consequently, the result which is valid for any combination of couplings and charges is independent of η^3.

In the vicinity of the event horizon of the extremal black hole the renormalized stress-energy tensor has the following expansion

$$96\pi^2 m^2 \langle T_a^b \rangle^{ABG} = t_a^{(1)b} + t_a^{(2)b}\,(x - x_{extr}) + \mathcal{O}\left(x - x_{extr}\right)^2, \tag{35}$$

$$t_t^{(1)t}=t_r^{(1)r}=-\frac{1}{4096}\,\frac{(1+w)^6\,(2+w)\,(w-1)^2\,\eta^3}{w^6M^6}-\frac{1}{245760}\,\frac{(1+w)^6\,(4+w+w^3+2\,w^2)\,\eta}{w^6M^6}$$
$$+\frac{1}{1935360}\,\frac{(1+w)^6\,(w^3+3\,w^2+3\,w+5)}{w^6M^6}, \tag{36}$$

$$t_t^{(2)t}=t_r^{(2)r}=\frac{3}{16384}\,\frac{(1+w)^7\,(w+3)\,(w^2-2\,w+1)\,\eta^3}{w^7M^6}-\frac{1}{2580480}\,\frac{(1+w)^7\,(w+3)\,(w^2+3)}{w^7M^6}$$
$$+\frac{1}{983040}\,\frac{(1+w)^7\,(w+3)\,(3\,w^2-2\,w+7)\,\eta}{w^7M^6}, \tag{37}$$

$$t_\theta^{(1)\theta}=t_\phi^{(1)\phi}=\frac{1}{8192}\,\frac{(1+w)^6\,(w+5)\,(w-1)^2\,\eta^3}{w^6M^6}+\frac{1}{491520}\,\frac{(1+w)^6\,(-w+13+3\,w^2+w^3)\,\eta}{w^6M^6}$$
$$-\frac{1}{3870720}\,\frac{(1+w)^6\,(3\,w+17+3\,w^2+w^3)}{w^6M^6} \tag{38}$$

and

$$t_\theta^{(2)\theta}=t_\phi^{(2)\phi}=-\frac{3}{32768}\,\frac{(1+w)^7\,(-25\,w+34-23\,w^2+9\,w^3+5\,w^4)\,\eta^3}{M^6w^7}$$
$$-\frac{1}{16384}\,\frac{(1+w)^7\,(-10\,w-8+w^2+4\,w^3+w^4)\,\eta^2}{M^6w^7}$$
$$+\frac{1}{1966080}\,\frac{(1+w)^7\,(-185\,w-190-111\,w^2+5\,w^4-15\,w^3)\,\eta}{M^6w^7}. \tag{39}$$

Since $\tilde{T}_a^{(1)b}$ vanishes in the limit $x\to x_{extr}$ there are no terms proportional to η^2 in (36–38).

The components of the stress-energy tensor of the massive scalar field are regular functions of the radial coordinate and are finite on the event horizon. Moreover, it could be demonstrated that the difference between radial and time components of $\langle T_a^b\rangle^{ABG}$ factorizes:

$$\langle T_t^t\rangle^{ABG}-\langle T_r^r\rangle^{ABG}=\left[1-\frac{2M}{r}\left(1-\tanh\frac{e^2}{2Mr}\right)\right]F\left(r\right), \tag{40}$$

where $F\left(r\right)$ is a regular function and, consequently, the stress-energy tensor is finite in a freely falling frame. To demonstrate this let us consider a slightly more general line element

$$ds^2=-f\left(x^1\right)\left(dx^0\right)^2+g\left(x^1\right)\left(dx^1\right)^2+\left(x^1\right)^2d\Omega^2. \tag{41}$$

For a radial motion the vectors of the frame are the four-velocity $e_0^\alpha=u^\alpha$ and a unit length spacelike vector $e_1^\alpha=n^\alpha$. Then, using the geodesic equation, one finds

$$e_{(0)}^a=u^a=\left(\frac{\gamma}{f},-\sqrt{\left(\frac{\gamma^2}{f}-1\right)\frac{1}{g}},0,0\right) \tag{42}$$

and

$$e^a_{(1)} = n^a = \left(-\frac{1}{f}\sqrt{\gamma^2 - f}, \frac{\gamma}{\sqrt{fg}}, 0, 0 \right), \tag{43}$$

where γ is the energy per unit mass along the geodesic. A simple calculation shows that the components $T_{(0)(0)}$, $T_{(0)(1)}$ and $T_{(1)(1)}$ in a freely falling frame (independent of the function $g\,(x^1)$) are

$$T_{(0)(0)} = \frac{\gamma^2(T^1_1 - T^0_0)}{f} - T^1_1, \tag{44}$$

$$T_{(1)(1)} = \frac{\gamma^2(T^1_1 - T^0_0)}{f} + T^1_1, \tag{45}$$

$$T_{(0)(1)} = -\frac{\gamma\sqrt{\gamma^2 - f}(T^1_1 - T^0_0)}{f}. \tag{46}$$

One concludes, therefore, that if all components of T^b_a and

$$\frac{(T^1_1 - T^0_0)}{f} \tag{47}$$

are finite on the horizon, the stress-energy tensor in a freely falling frame is finite as well. It is expected that constructed formulas satisfactorily approximate the exact stress-energy tensor. On the other hand however, to establish the regularity of the exact $\langle T^b_a \rangle^{ABG}$ in a freely falling frame one has to explicitly demonstrate that (47) is satisfied.

IV. NUMERICAL RESULTS

Considerations of the previous section are limited to analytically tractable special cases. However, to gain insight into the overall behavior of the stress-energy tensor for any combination of couplings and charges one has to refer to numerical calculations — our complete but rather complicated analytical formulas are, unfortunately, not of much help in this regard. Below we describe the main features of the constructed tensors and present them graphically, fixing our attention on the physically interesting case of minimal coupling. Related plots showing the radial dependence of C^b_a and $T^{(0)b}_a$ can be found in Ref. [16], where the discussion of the stress-energy tensor of the massive scalar field with conformal coupling with curvature has been carried out.

The case of arbitrary η is much more complicated as the tensor $\langle T^b_a \rangle^{ABG}$, given by (5), is modified by the presence of additional terms. However, numerical analysis performed for $\eta = -1/6$ reveals that the contribution of $\eta^3 T^{(3)b}_a$ is neglegible for q even as large as 1.0. Moreover, a closer examination indicates that as one approaches the extremality limit, the magnitude of this very term becomes comparable with $\eta^2 T^{(2)b}_a$ and $\eta T^{(1)b}_a$ only in the closest vicinity of the event horizon. Our calculations also suggest that irrespective of the exact value of q, each component of $T^{(1)b}_a$ is a monotonic function of the radial coordinate in a large neighbourhood of the event horizon, if not in the whole range $r > r_+$. For the extremal case

such a behaviour is illustrated in Figs. 1–3, where the time, radial, and angular components of $T_a^{(1)b}$ are displayed. For comparison and completeness we also present the run of $T_a^{(0)b}$, C_a^b, and D_a^b, where the latter two tensors have been calculated for the RN line element with the aid of Eqs. (20–25). It should be noted that even in the extremal case, when the differences between two considered geometries are most prominent, the tensors $T_a^{(1)b}$ and D_a^b behave in a similar manner though differing noticeably in magnitude. For small values of q, the curves constructed for both types of black hole are almost indistinguishable, which could be easily established from Eq. (27).

On the other hand however, the components of $T_a^{(2)b}$ exhibit quite different but very regular behavior, which will be described in some detail. For $q \ll 1$ it can be, of course, inferred from the approximate formulas (27–30); greater values of q require numerical examination. Specifically, for small charges each component of the considered tensor is negative at $r = r_+$, and before approaching zero as $r \to \infty$, it changes sign once for the radial component and twice for time and angular components. With the increase of q, all components become strongly negative at r_+, with their zeros shifted towards larger values of the radial coordinate. Near the extremality limit, the tensor $T_a^{(2)b}$ is very sensitive to changes of q, which is illustrated in Figs. 4–6. If the value of ratio $|e|/M$ slightly exceeds 1.0, for all components there occurs a negative minimum not far away from the event horizon. For the extremal ABG black hole $T_a^{(2)b}$ vanishes at r_+, as is clearly seen from Eqs. (35–38), and exhibits oscillatory-like behavior with a rapidly decreased amplitude and increased intervals between zeros. The angular component attains a very distinct maximum near the event horizon whereas for time and radial component there are minima close to r_+.

The competition of the terms described above results in the overall behaviour of the stress-energy tensor of minimally coupled massive fields in the geometry of the ABG black hole. Numerical calculations indicate that for small and intermediate values of q, up to about 0.8, $\langle T_a^b \rangle^{ABG}$ still resembles that evaluated for conformal coupling. For larger values of q, however, the change of curvature coupling leads to a considerable modification of the results as both magnitudes and radial variations become significantly different. This is illustrated in Figs. 7–9, where values of q at and near the extremality limit were chosen. The oscillatory-like behaviour of $T_a^{(2)b}$ for q close to q_{extr} is refected by the presence of local extrema visible in the stress-energy tensor, and, for the angular component, an inflection point. It is in a sharp contrast with the almost monotonic behavior of the stress-energy tensor of conformally coupled massive fields depicted in Fig. 7–9 by the dashed lines. Moreover, it should be noted that for $\eta = -1/6$, when the extremality limit is approached, there are substantial changes of values of $\langle T_a^b \rangle^{ABG}$ at the event horizon as well as in the behavior of the stress-energy tensor in a narrow strip near r_{extr}. There appear also certain new features for the time and radial components which are not present in the case of the conformal coupling. Indeed, for $0.987 \lesssim q \lesssim 1.032$, the energy density $\rho = -\langle T_t^t \rangle^{ABG}$ is positive at the event horizon whereas for the same values of q, the horizon value of the radial pressure $p_r = \langle T_r^r \rangle^{ABG}$ is negative. It should be noted in this regard that for $\eta = 0$ the radial component of the stress-energy tensor is always positive there. On the other hand, the angular pressure is positive on the event horizon for $|e|/M \lesssim 0.922$ and negative for larger values that is very similar to the previously studied case of conformal coupling.

V. CONCLUDING REMARKS

In this work our goal was to construct the renormalized stress-energy tensor of the quantized massive field in the spacetime of a nonlinear black hole and to investigate how the choice of the curvature coupling affects the results. A regular electrically charged solution of this type has been recently proposed by Ayón-Beato and García in $\mathcal{P}$ formulation of nonlinear electrodynamics and reinterpreted by Bronnikov as a regular magnetically charged solution of the standard $\mathcal{F}$ formulation. For small and intermediate values of the ratio $|e|/M$ the metric structure of the nonlinear solution closely resembles that of Reissner and Nordström and the similarities in the line elements are reflected in the behavior of the stress-energy tensor of the conformally coupled massive scalar fields; notable differences appear near and at the extremality limit.

As the general $\langle T_a^b \rangle^{ABG}$ contains terms that are quadratic and cubic in η, the case of arbitrary coupling is more complicated. Again, for small and intermediate values of q there is a similarity between the $\langle T_a^b \rangle$ evaluated for the minimally coupled scalar field in the ABG geometry and its RN counterpart. Modifications for q slightly exceeding 0.8, which are mainly due to the term $T_a^{(2)b}$, are noticeable although there are still some similarities. Comparison of $\langle T_a^b \rangle^{ABG}$ for charges close to q_{extr} indicates that the radial dependences for both couplings are completely different. Indeed, the behaviour of the stress-energy tensor for the minimal coupling is far more complicated as compared with its almost monotonic radial dependence for $\eta = 0$. Moreover, the former is even more sensitive to changes of q, especially near the extremality limit. In addition, new features occur as, for example, positivity of the energy density at the event horizon for certain values of q.

It should be emphasized, that being local the Schwinger-DeWitt approximation does not describe particle creation, and, therefore, it must not be applied in strong or rapidly varying gravitational fields. However, it is expected that for sufficiently massive fields the method provides a good approximation of the exact renormalized stress-energy tensor.

Finally, we remark that although complicated, the derived stress-energy tensor may be employed as a source term of the semi-classical Einstein field equations. Indeed, preliminary calculations indicate that it is possible to find an analytical perturbative solution to the back reaction, and what makes this issue even more interesting and worth further studies is the regularity of the geometry of the ABG black hole. We intend to return to this group of problems elsewhere.

REFERENCES

[1] B. A. Taylor, W. A. Hiscock, and P. R. Anderson, Phys. Rev. D **61**, 084021 (2000).
[2] J. W. York, Phys. Rev. D **31**, 775 (1985).
[3] C. O. Lousto and N. Sanchez, Phys. Lett. **B212**, 411 (1988).
[4] D. Hochberg and T. W. Kephart, Phys. Rev. D **47**, 1465 (1993).
[5] D. Hochberg, T. W. Kephart, and J. W. York, Phys. Rev. D **48**, 479 (1993).
[6] D. Hochberg, T. W. Kephart, and J. W. York, Phys. Rev. D **49**, 5257 (1994).
[7] P. R. Anderson, W. A. Hiscock, J. Whitesell, and J. W. York, Phys. Rev. D **50**, 6427 (1994).
[8] J. Matyjasek, Acta Phys. Polon. **B** 29, 529 (1998).
[9] V. P. Frolov and A. I. Zel'nikov, Phys. Lett. B **115**, 372 (1982).
[10] V. P. Frolov and A. I. Zel'nikov, Phys. Lett. B **123**, 197 (1983).
[11] V. P. Frolov and A. I. Zelnikov, Phys. Rev. D **29**, 1057 (1984).
[12] I. G. Avramidi, Ph.D. thesis, Moscow State University, (hep-th/9510140).
[13] I. G. Avramidi, Theor. Math. Phys. **79**, 494 (1989).
[14] I. G. Avramidi, Nucl. Phys. **B355**, 712 (1991).
[15] J. Matyjasek, Phys. Rev. D **61**, 124019 (2000).
[16] J. Matyjasek, Phys. Rev. D **63**, 084004 (2001).
[17] P. R. Anderson, W. A. Hiscock, and D. A. Samuel, Phys. Rev. D **51**, 4337 (1995).
[18] B. A. Taylor, W. A. Hiscock, and P. R. Anderson, Phys. Rev. D **55**, 6116 (1997).
[19] K. A. Bronnikov, V. N. Melnikov, G. N. Shikin, and K. P. Staniukowicz, Annals Phys. **118**, 84 (1979).
[20] E. Ayón-Beato and A. García, Phys. Lett. **B464**, 25 (1999).
[21] K. A. Bronnikov, Phys. Rev. D **63**, 044005 (2001).
[22] A. Burinsky and S. R. Hildebrandt, New type of regular black holes and particlelike solutions from Nonlinear Electrodynamics,(hep-th/0202066).
[23] I. H. Salazar, A. Garcia, and J. Plebanski, J. Math. Phys. **28**, 2171 (1987).
[24] K. A. Bronnikov, Phys. Rev. Lett. **85**, 4641 (2000).
[25] M. Novello, S. E. Perez Bergliaffa, and J. S. Salim, Class. Quantum Grav. **17**, 3821 (2000).
[26] M. Novello, V. A. De Lorenci, J. S. Salim, and R. Klippert, Phys. Rev. D **61**, 045001 (2000).
[27] M. Novello, S. E. Perez Bergliaffa, and J. S. Salim, Phys. Rev. D **63**, 083511 (2001).
[28] R. M. Corless *et al.*, Adv. Comput. Math. **5**, 329 (1996).

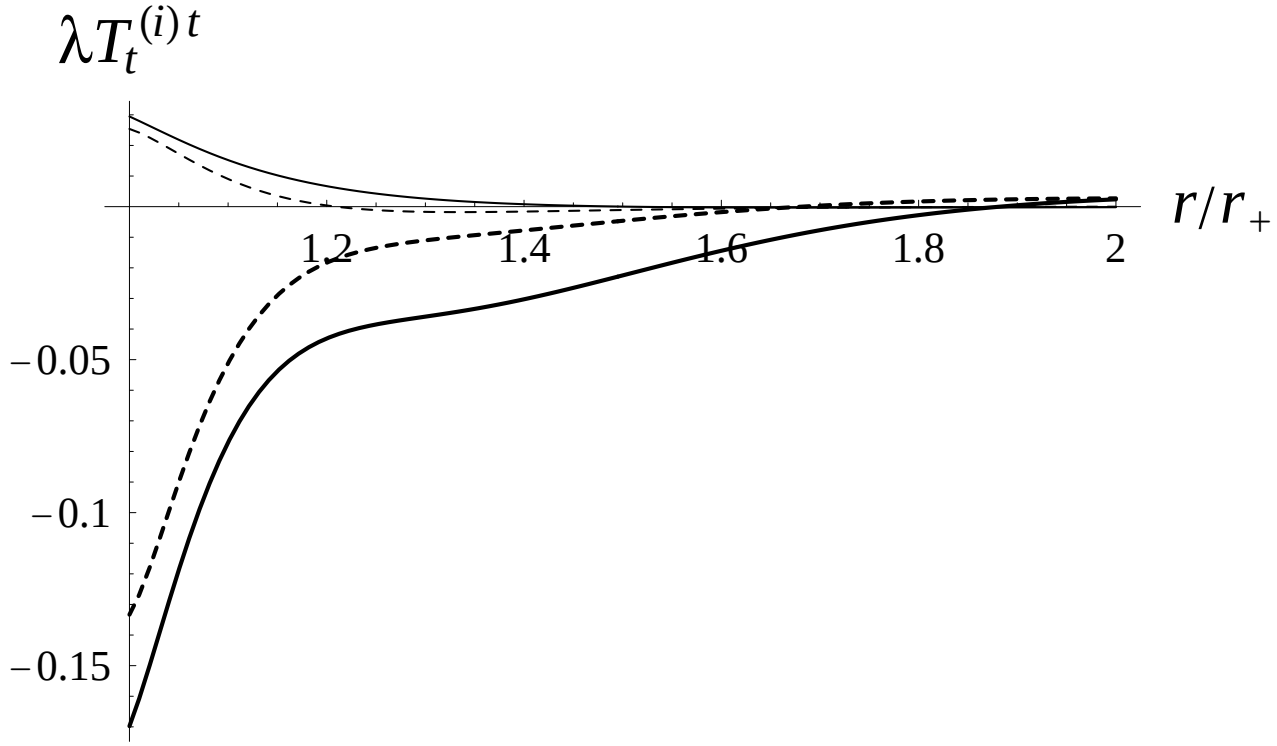

FIG. 1. The radial dependence of the rescaled time component $\lambda T_t^{(1)t}$ ($\lambda = 96\pi^2 M^6 m^2$) (solid thick line) and $\lambda T_t^{(0)t}$ (solid thin line) contributing to the renormalized stress-energy tensor of the massive scalar field for the extremal ABG geometry. The dashed lines correspond to the appropriate tensors for extremal RN black hole: λC_t^t (thin curve) and λD_t^t (thick curve).

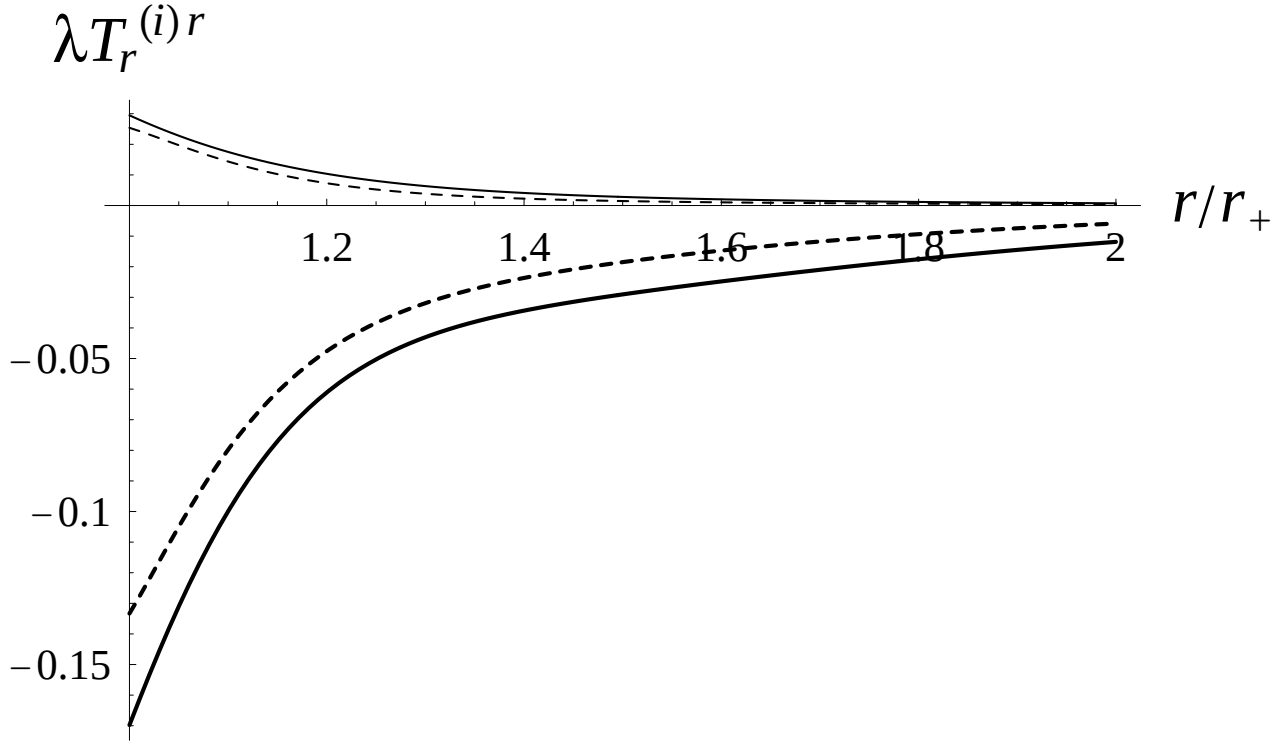

FIG. 2. The radial dependence of the rescaled radial component $\lambda T_r^{(1)r}$ ($\lambda = 96\pi^2 M^6 m^2$) (solid thick line) and $\lambda T_r^{(0)r}$ (solid thin line) contributing to the renormalized stress-energy tensor of the massive scalar field for the extremal ABG geometry. The dashed lines correspond to the appropriate tensors for extremal RN black hole: λC_r^r (thin curve) and λD_r^r (thick curve).

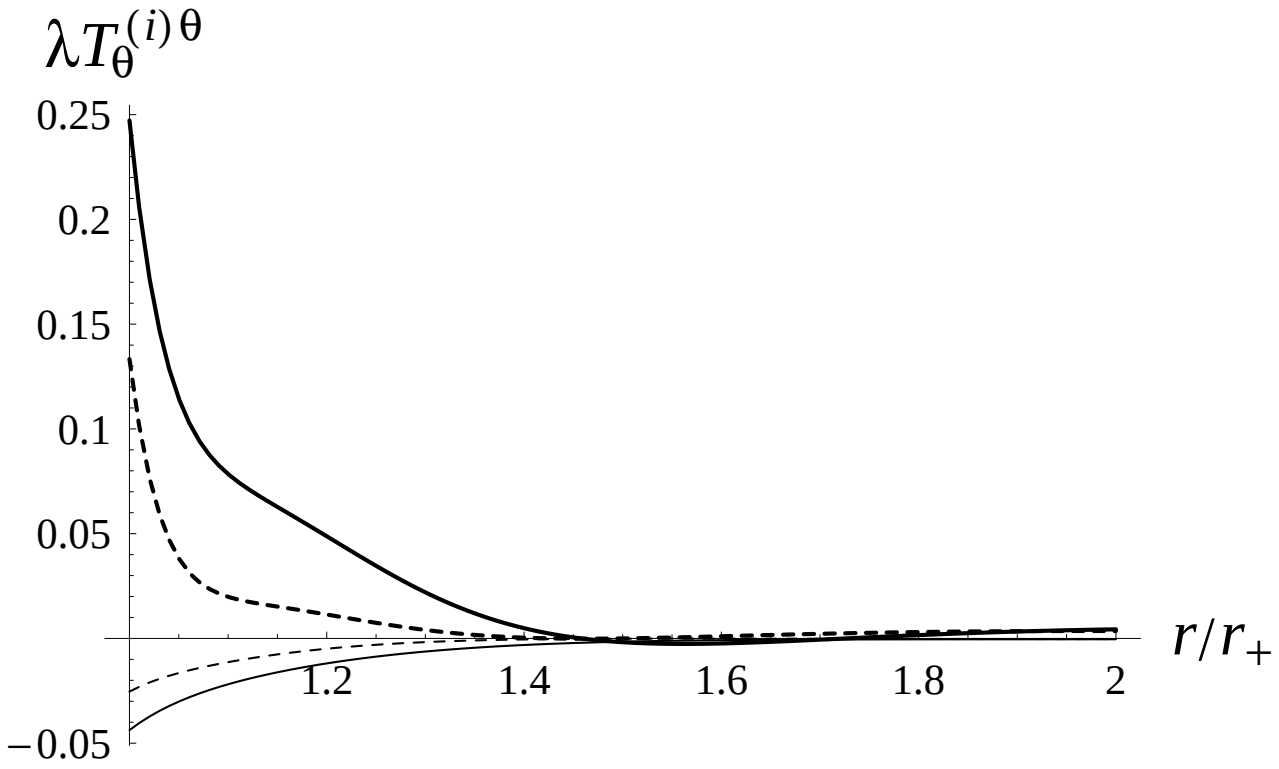

FIG. 3. The radial dependence of the rescaled angular component $\lambda T_{\theta}^{(1)\theta}$ ($\lambda = 96\pi^2 M^6 m^2$) (solid thick line) and $\lambda T_{\theta}^{(0)\theta}$ (solid thin line) contributing to the renormalized stress-energy tensor of the massive scalar field for the extremal ABG geometry. The dashed lines correspond to the appropriate tensors for extremal RN black hole: $\lambda C_{\theta}^{\theta}$ (thin curve) and $\lambda D_{\theta}^{\theta}$ (thick curve).

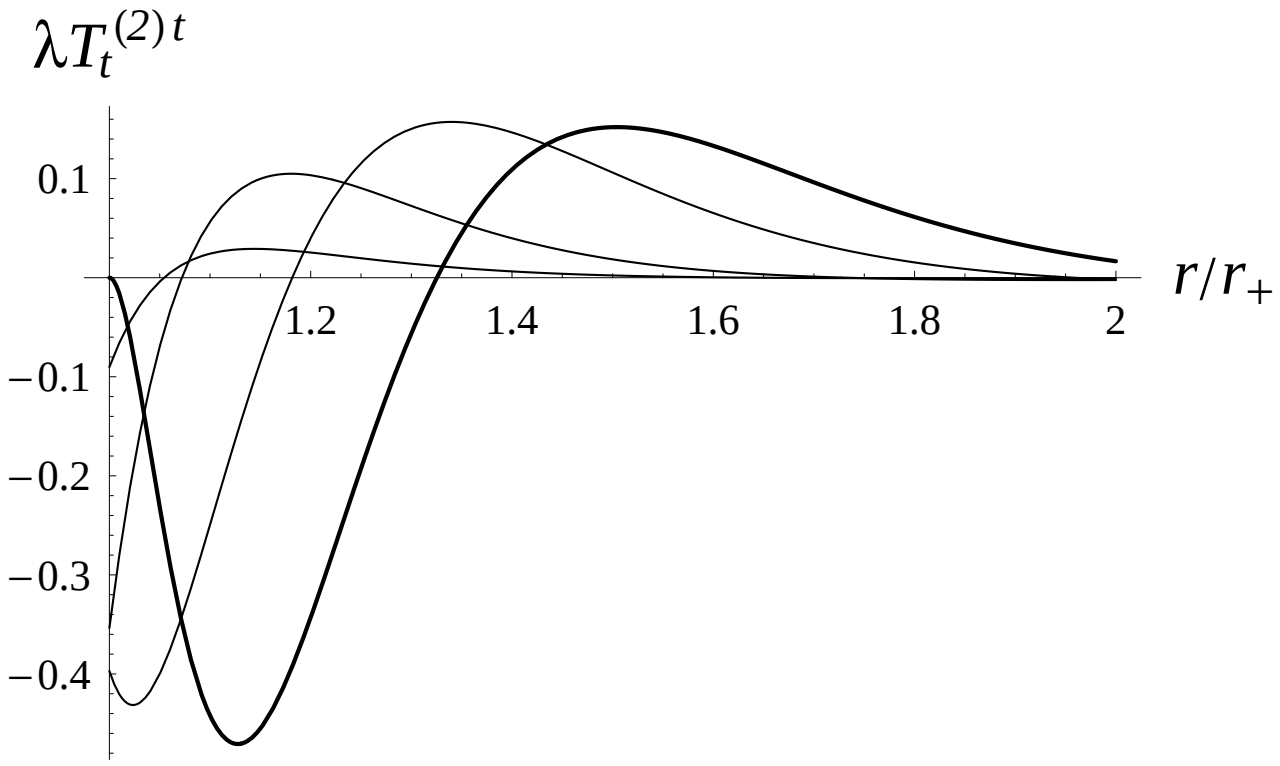

FIG. 4. The radial dependence of the rescaled time component $\lambda T_t^{(2)t}$ ($\lambda = 96\pi^2 M^6 m^2$) contributing to the renormalized stress-energy tensor of the arbitrarily coupled massive scalar field in the ABG geometry. The thick curve corresponds to the extremal case and the thin curves are for a series of q values approaching the extremality limit, $q = 0.9, 1, 1.05$.

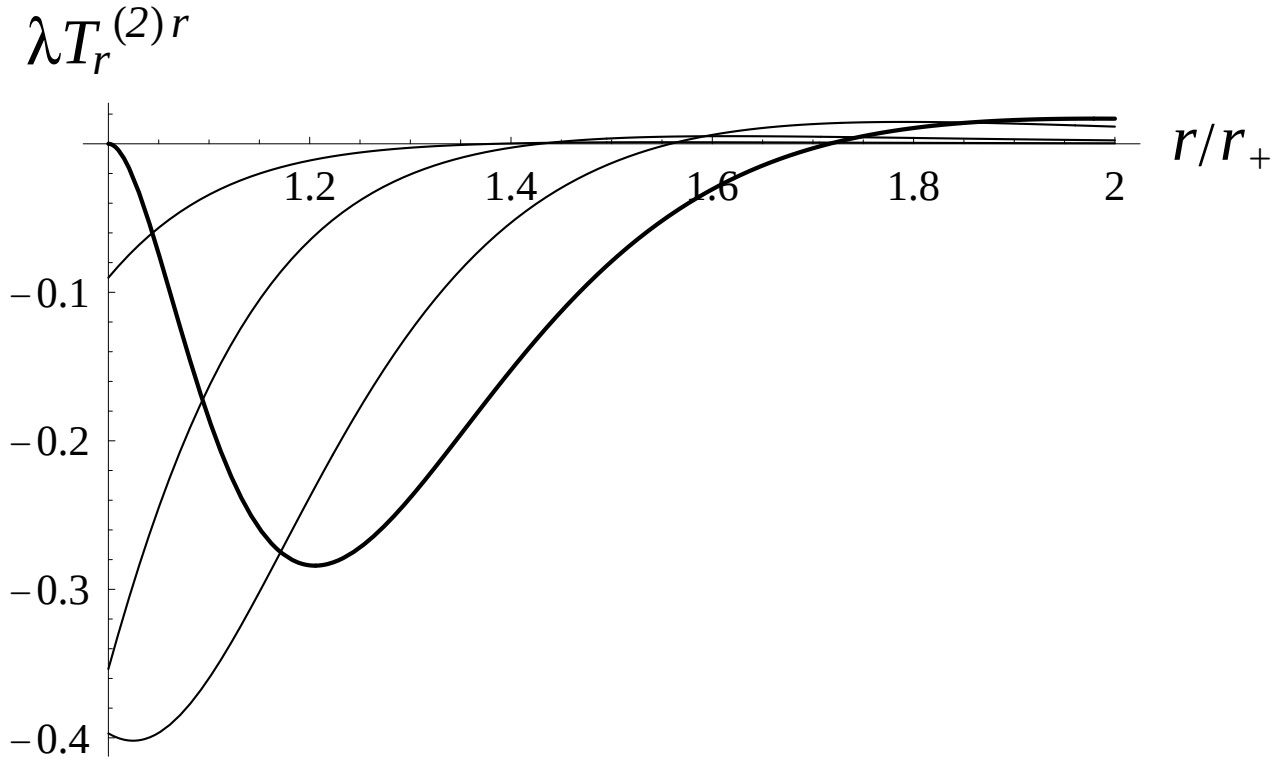

FIG. 5. The radial dependence of the rescaled radial component $\lambda T_r^{(2)r}$ ($\lambda = 96\pi^2 M^6 m^2$) contributing to the renormalized stress-energy tensor of the arbitrarily coupled massive scalar field in the ABG geometry. The thick curve corresponds to the extremal case and the thin curves are for a series of q values approaching the extremality limit, $q = 0.9, 1, 1.05$.

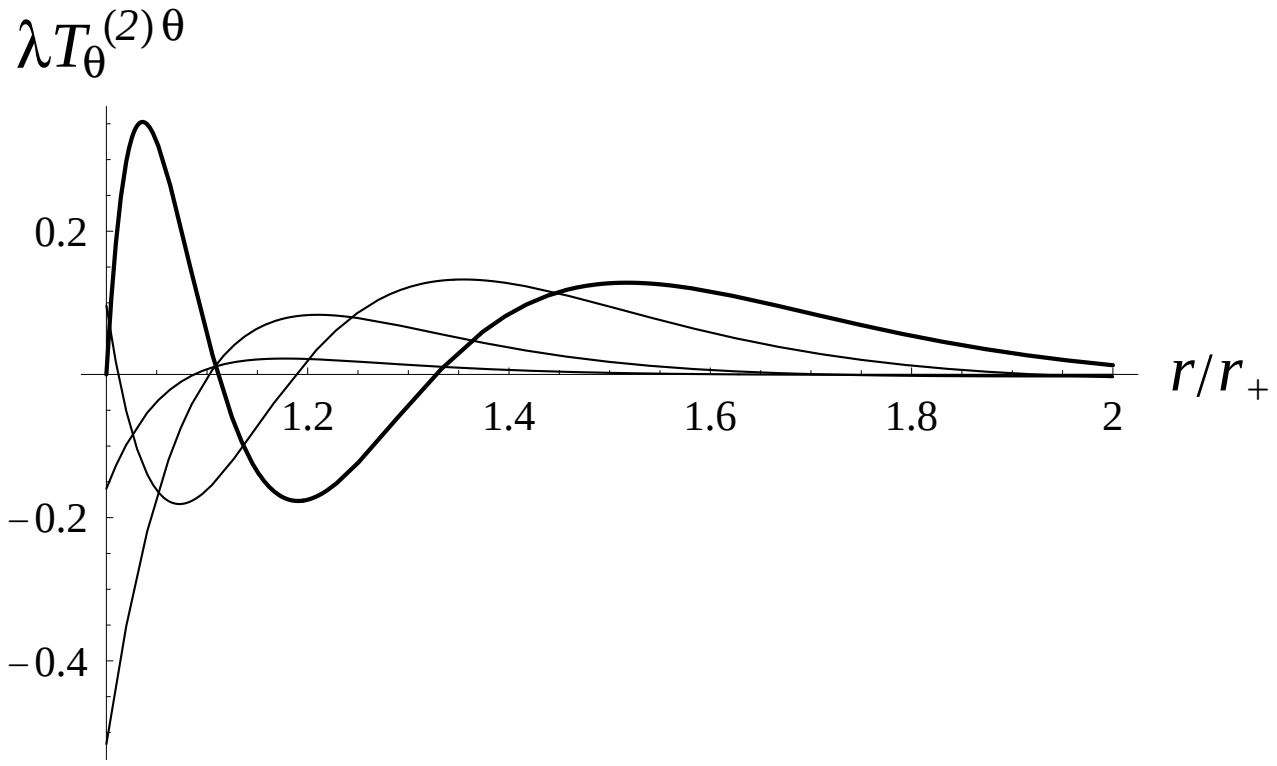

FIG. 6. The radial dependence of the rescaled angular component $\lambda T_{\theta}^{(2)\theta}$ ($\lambda = 96\pi^2 M^6 m^2$) contributing to the renormalized stress-energy tensor of the arbitrarily coupled massive scalar field in the ABG geometry. The thick curve corresponds to the extremal case and the thin curves are for a series of q values approaching the extremality limit, $q = 0.9, 1, 1.05$.

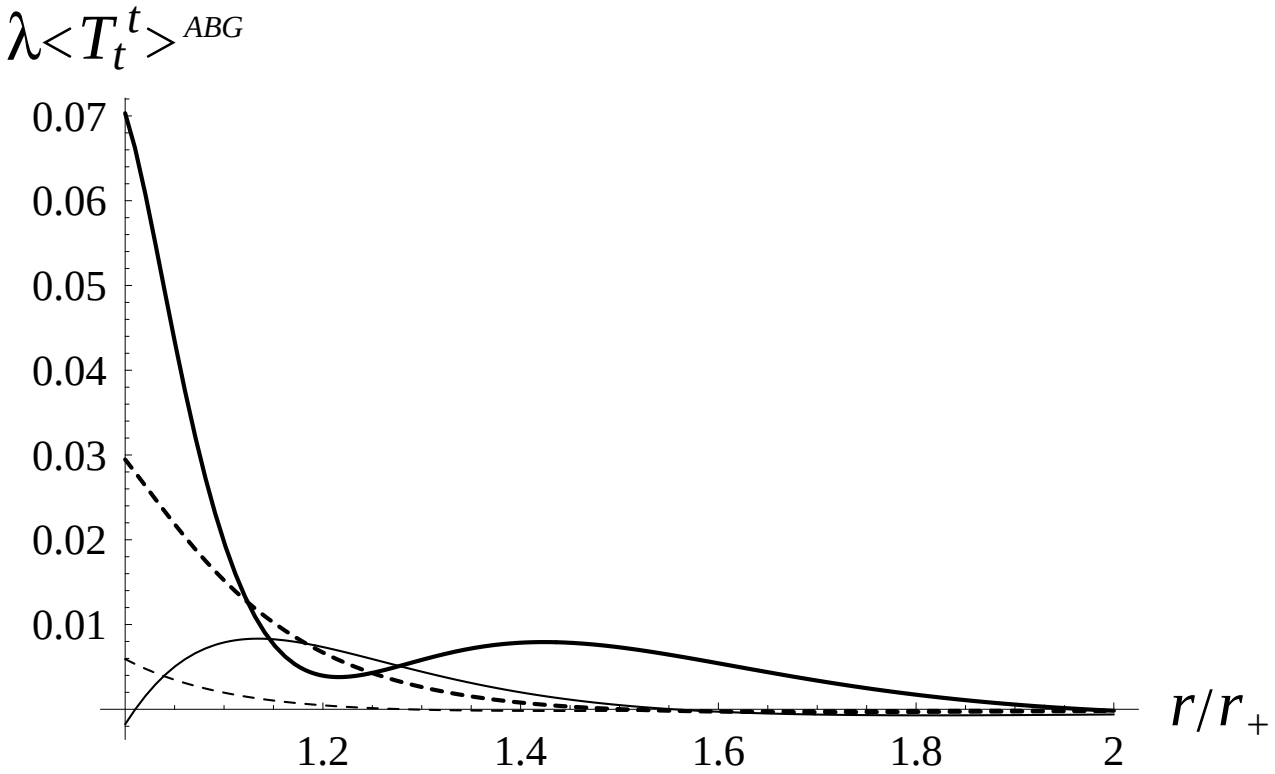

FIG. 7. The radial dependence of the rescaled time component $\lambda\langle T_t^t\rangle^{ABG}$ ($\lambda = 96\pi^2 M^6 m^2$) of the renormalized stress-energy tensor of the minimally coupled massive scalar field in the ABG geometry solid lines) as compared to the case of conformal coupling in this geometry (dashed lines). The thin curves are for $q = 1.02$ and the thick curves are for the extremal case.

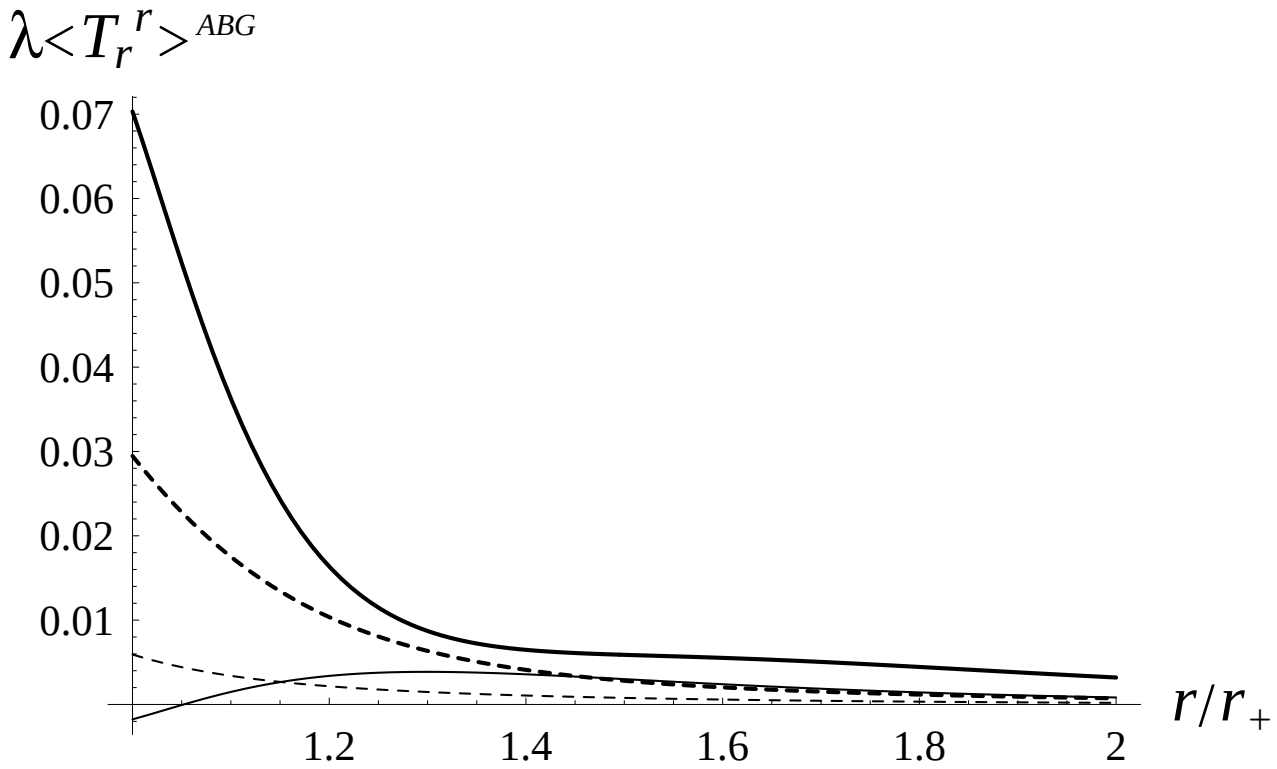

FIG. 8. The radial dependence of the rescaled radial component $\lambda\langle T_r^r\rangle^{ABG}$ ($\lambda = 96\pi^2 M^6 m^2$) of the renormalized stress-energy tensor of the minimally coupled massive scalar field in the ABG geometry (solid lines) as compared to the case of conformal coupling in this geometry (dashed lines). The thin curves are for $q = 1.02$ and the thick curves are for the extremal case.

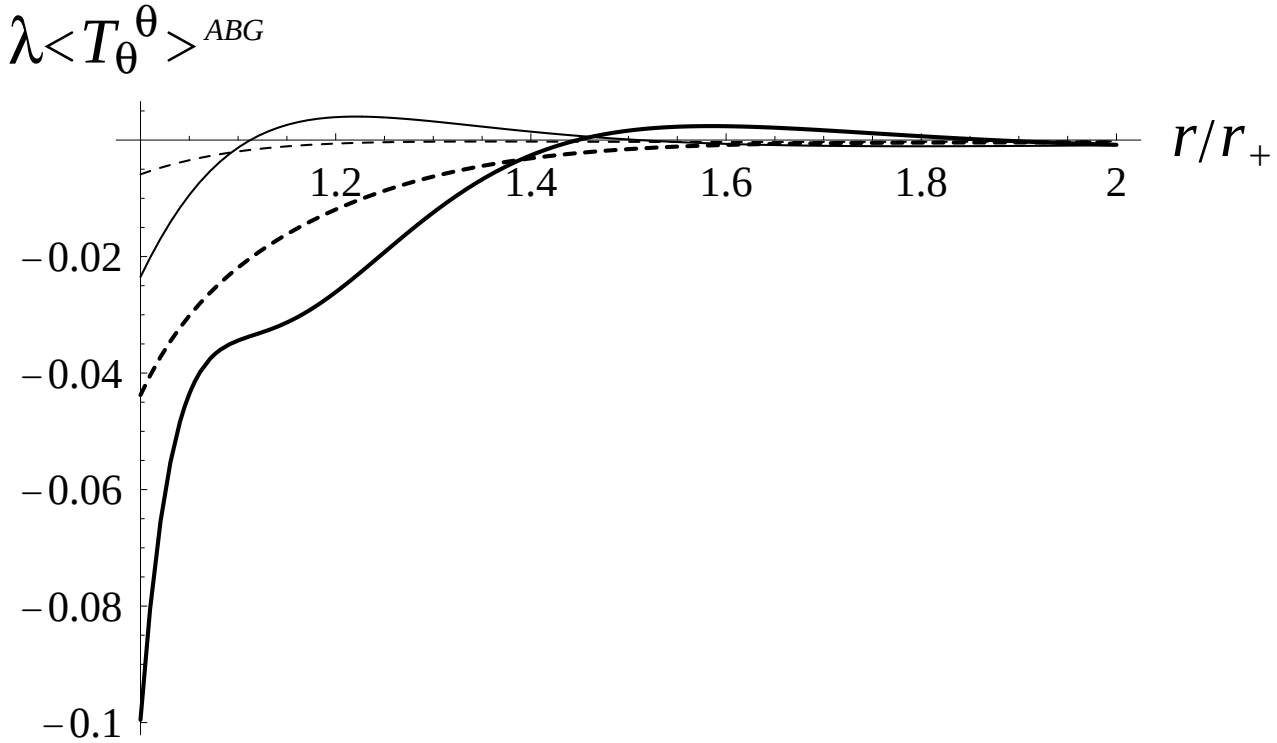

FIG. 9. The radial dependence of the rescaled angular component $\lambda\langle T^{\theta}_{\theta}\rangle^{ABG}$ ($\lambda = 96\pi^2 M^6 m^2$) of the renormalized stress-energy tensor of the minimally coupled massive scalar field in the ABG geometry (solid lines) as compared to the case of conformal coupling in this geometry (dashed lines). The thin curves are for $q = 1.02$ and the thick curves are for the extremal case.